Desalination and Water Treatment
www.deswater.com

doi: 10.1080/19443994.2015.1136694

57 (2016) 22632–22645
October

Taylor & Francis
Taylor & Francis Group

Development of novel chitosan schiff base derivatives for cationic dye removal: methyl orange model

E.M. El-Sayed[a], T.M. Tamer[b], A.M. Omer[b], M.S. Mohy Eldin[b,c,*]

[a]*Fabrication Research Department Advanced Technologies and New Materials Research Institute, City of Scientific Research and Technological Applications, New Borg El-Arab City, 21934 Alexandria, Egypt, email: eng.cinderella@yahoo.com*
[b]*Polymer Materials Research Department, Advanced Technologies and New Materials Research Institute, City of Scientific Research and Technological Applications, New Borg El-Arab City, 21934 Alexandria, Egypt, emails: ttamer85@yahoo.com (T.M. Tamer), ahmedomer_81@yahoo.com (A.M. Omer), m.mohyeldin@mucsat.sci.eg (M.S. Mohy Eldin)*
[c]*Faculty of Science, Chemistry Department, University of Jeddah, Osfan P.O. Box 80203, Jeddah 21589, Saudi Arabia*

Received 24 June 2015; Accepted 5 December 2015

ABSTRACT

Adsorption of anionic reactive dye (methyl orange) onto cross-linked Chitosan derivate Schiff bases obtained from the coupling of Chitosan with 1-vinyl 2- pyrrolidone [Schiff base (I)] and 4-amino acetanilide (Schiff base (II)) in aqueous solutions was investigated using batch mode under various parameters. The structure of the prepared new Schiff bases was characterized using FT-IR and thermal gravimetric analysis. A batch experiment was conducted to study the process of Methyl orange dye adsorption from aqueous solutions using new Chitosan Schiff bases (I) and (II) comparing to cross-linked Chitosan. The influence of contact time, initial dye concentration, temperature, system pH, agitation speed, and adsorbent dosage on dye adsorption investigated. The experimental results showed that the maximum % dye removal obtained at pH 7 (pH 8 in the case of Schiff base (I)), temperature 80°C, 250 rpm, and contact time 70 min. The adsorption equilibrium data analyzed by Langmuir and Freundlich isotherm models. Langmuir model describes the equilibrium information and fitted perfectly. The experimental kinetics data were well suited and found that the kinetics of the removal of methyl orange dye using the prepared sorbents follows a pseudo-first-order model.

Keywords: Chitosan; Schiff base; TGA; Methyl orange; Dye removal

1. Introduction

Global needs for water and the limited available resources pay the attention to the search for untraditional resources of water and improve the use water managements. Reuses of wastewater, especially the industrial one, provide a valuable perspective for better management. Excessive amounts of water used by many industries that excreted colored water as waste at the end. Losing transparency and acquired color are the main contamination parameter to describe wastewater [1]. Only a few milligrams of dyes in water causes such contamination [1,2]. Main three categories of dyes produced commercially namely; anionic (direct, acidic, and reactive), cationic (alkaline), and non-ionic (suspensions). The anionic one had the greatest contribution to the market (30%) due to

*Corresponding author.

1944-3994/1944-3986 © 2016 Balaban Desalination Publications. All rights reserved.

excellent characters for industrial application [3,4], and varied range of materials can dye such as wool, cotton, nylon, and silk [5]. Some of the materials show the low capability to dyeing resulted in losing from 10 to 50% of reactive anionic dyes in wastewaters during the dyeing process [6]. The central component of their structure is aromatic rings, so such dyes are not subjected to biodegradation easily. Also, further toxic and even carcinogenic impacts of these dyes type induced serious hazard to aquatic living organisms [7,8].

Since it can be used to remove different types of coloring materials among numerous techniques of dye removal, so adsorption comes to be the procedure of choice [9,10]. Although activated carbon is a preferred sorbent, its global usage is restricted due to its high cost. The trying of different strategies to find inexpensive alternative adsorbents is the main goal in designing the treatment system. Recently, different approaches were investigated to develop economical adsorbents. Natural materials, bio-sorbents, and waste materials from industry and agriculture proposed as non-conventional low-cost adsorbents. Different matrices reported for dyes removal application such as clay materials [10–16], zeolites [17–25], agricultural wastes, industrial waste products, [26–33]. Bio-Sorbents such as Chitosan, peat, biomass and carbohydrates such as starch, cyclodextrin, and cotton were investigated [34–39].

Chitosan is a poly glucosamine biopolymer. It's coming after cellulose as the most abundant polysaccharide acquiring economically attractive due to production from renewable commercial source as the skeleton of Marine crustaceans. As an adsorbent for transition metal ions, organic species as well as colored material studies, it showed a higher capacity for adsorption than activated carbon.

Having different function groups like amino (NH_2) and hydroxyl (OH) groups along its backbone induced simple chemical transformation and modifications [40–43]. Among these modifications, Schiff bases that obtained by reaction of free amino groups of Chitosan with active carbonyl compounds such as aldehyde or ketone considered the most easily transformation [44,45]. The obtained (–RC=N–) groups of these Schiff bases offer several potential analytical and environmental applications by enhancing the adsorption/complexation properties [46,47].

2. Materials and methods

2.1. Materials

Shrimp skeleton collected from a domestic source, sodium hydroxide (NaOH), acetic acid (CH_3COOH), methyl orange dye (MO), 1-vinyl 2- pyrrolidone, and 4-amino acetanilide purchased from Sigma–Aldrich.

2.2. Preparation and characterization of the adsorbents

2.2.1. Extraction of chitin from shrimp Shells

According to the published results [48], the process carried out through the following steps: Demineralization of Shells, in this step, the shells was dispersed in 5% HCl at room temperature in the ratio of 1:14 (w/v) overnight. After 24 h, the shells were quite squishy and were rinsed using water to remove acid and calcium chloride. The de-mineralized shells were then treated with 5% NaOH at room temperature for 24 h in the ratio of 12:1 (v/w). The residue was then collected and washed to neutrality in running tap water and then distilled water. The obtained product is chitin.

2.2.2. Preparation of chitosan from chitin

According to previously published method [49], preparation of Chitosan simply is a deacetylation of chitin in alkaline medium. Removal of acetyl groups from the chitin achieved by using 50% NaOH solution with a solid to solution ratio of 1:50 (w/v) at 100–120˚C for 12 h. The resulting Chitosan washed to neutrality with distilled water.

2.2.3. Preparation of Chitosan Schiff base hydrogel

Crosslinked Chitosan Schiff base was prepared according to the published modification protocol [50]. In details, (31 mMole) of the prepared Chitosan was dissolved in 200 mL acetic acid solution (2%) at ambient temperature overnight. Filtration of Chitosan solution carried out using cheesecloth to remove un-dissolved Chitosan. Then a certain amount of absolute ethanol was added to Chitosan solution; with continuous stirring to have a homogenous solution. 31 mM of 1-vinyl 2- pyrrolidone (I) or 4-amino acetanilide (II) that previously dissolved in 20 ml ethanol added to above solution. After that, the temperature rose to 80˚C, the reaction mixture was left to react under continuous stirring, at the end of 3 h, 5 ml of 25% glutaraldehyde added to the reaction medium and kept at reaction conditions for another 1 h. Finally, the obtained gels were collected by filtration, washed several times with ethanol to remove any unreacted aldehydes, and dried at 60˚C under reduced pressure.

2.3. Characterization

2.3.1. Infrared Spectrophotometric

Infrared spectra were performed with Fourier Transform Infrared Spectrophotometer (Shimadzu FTIR–8400 S, Japan) to confirm modification and prove the structure of Chitosan and its two different derivatives.

2.3.2. Thermal gravimetric analysis

Analysis by Thermal gravimetric analysis (TGA) of Chitosan and the two different derivatives were carried out using Thermogravimetric Analyzer (Shimadzu TGA–50, Japan) under Nitrogen to evidence changes in structure as a result of the modification. Samples moisture content were first measured their weight loss starting from room temperature to 120˚C at a heating rate of 10˚C per minute. Then, cooled and reanalyzed again from room temperature to 600˚C.

2.4. Batch equilibrium studies

A stock solution of 1 g/L of MO dye (1,000 ppm) was prepared by dissolving appropriate amount of dye in distilled water then the used concentrations were obtained by dilution. All the adsorption experiments were conducted in 100 mL flasks by adding a given amount of adsorbent to 25 mL dye solution of different concentrations with different pH value and shaking on an orbital shaker for a given time. The adsorbate concentrations of the initial and final aqueous solutions were measured using UV–vis spectrophotometer at 464 nm. The amount of dye adsorbed was calculated from the difference between the initial concentration and the equilibrium one. The values of percentage removal and amount of dye adsorbed were calculated using the following relationships:

$$\text{Dye adsorption } \% = (C_0 - C_e)/C_0 \times 100\% \quad (1)$$

where C_0 is the initial dye concentration and C_e is the final dye concentration in supernatant.

2.5. Adsorption isotherms

Equilibrium data, commonly known as adsorption isotherms, is fundamental importance in the design of adsorption systems. The isotherm expresses the relation between the mass of the dye adsorbed at a particular temperature, the pH, particle size, and liquid phase of the dye concentration. For any adsorption investigation, one of the most important parameters required to understand the behavior of the adsorption process in the adsorption isotherm.

The shape of an isotherm not only provides information about the affinity of the dye molecules for adsorption, but it also reflects the possible mode for adsorbing dye molecules. The most common way of obtaining an adsorption isotherm is to determine the concentration of the dye solution before and after the adsorption experiments several attempts have been made to find the adsorbed amount. Several isotherm equations have been developed and employed for such analysis and the two important isotherms, the Langmuir, and Freundlich isotherms applied in this study.

2.5.1. Langmuir's isotherm

Langmuir's isotherm used for monolayer adsorption onto a surface containing a finite number of identical sites, and assumes uniform energies of adsorption on the surface, in addition to no transmigration of the adsorbate in the plane of the surface [51–53]. The Langmuir isotherm model determines the maximum capacity of the adsorbent from complete monolayer coverage of the adsorbent surface. The Langmuir isotherm [51] is represented by the following linear equation:

$$C_e/q_e = (1/q_m K) + (1/q_m) \quad (2)$$

where q_e is the solid-phase concentration in equilibrium with the liquid-phase concentration C_e, q_m is the final sorption capacity (most commonly in mg/mg), and K is an equilibrium constant (most commonly used in L/mg). The units of K are L/mol provided that C_e expressed in (mol/L).

2.5.2. Freundlich isotherm

Adsorbents that follow the Freundlich isotherm equation are assumed to have a heterogeneous surface consisting of sites with different adsorption potentials [54–56], and each type of site is assumed to adsorb molecules, as in the Langmuir equation:

$$q_e = K_f C_e^n \quad (3)$$

where q_e is the solid-phase concentration in equilibrium with the liquid-phase concentration C_e, K_f is constant (a function of the energy of energy of adsorption and temperature), and n is a constant. Freundlich iso-

therm was shown later to have some thermodynamic justification. Where rearranging equation above in the following form:

$$\ln q_e = \ln K_f + n \ln C_e \quad (4)$$

A straight line obtained when plotting ln q_e against ln C_e, which serves to evaluate the constants; K_f and n.

2.6. Kinetic studies

Kinetic experiments made by using 25 mL dye solutions of various concentrations (50, 75, 100 mg/L). Samples take at different time intervals (0–70 min), and remaining dye concentrations were analyzed. The rate constants were calculated using conventional rate expressions. Following formula was used to determine adsorbed MO amounts (q_t):

$$q_t = (C_o - C_t) \times V/m \quad (5)$$

where q_t (mg/g) is the adsorption capacity at time t, C_o (mg/L) is the initial MO concentration, and C_t (mg/L) is the concentration of MO in solution at time t. V (L) is the solution volume, and m (g) is the amount of the adsorbent.

3. Results and discussion

Novel Chitosan Schiff bases prepared and cross-linked with glutaraldehyde used for dye removal from aqueous solutions (see Figs. 1–3).

3.1. Characterization of prepared Chitosan derivatives

3.1.1. FT-IR spectroscopy

The FT-IR spectrum of Chitosan and Chitosan Schiff bases (I, II) resin presented in Fig. 4.

The figure demonstrates a broadband at 3,200–3,600 cm^{-1} corresponds to the stretching vibration of $–NH_2$ and OH groups of Chitosan. A new band generated at 1634.3 cm^{-1} attributed to –C=N vibration that confirmed the formation of Schiff bases. 1,171, 1,072.4, 1357 cm^{-1} bands resulting from C–O and C–O–C vibration were recognized. The peak at 1,330 cm^{-1} is due to –C–N– stretching in 1-vinyl 2-pyrrolidone overlapped with that at 1,357 cm^{-1} for Schiff base S(I). On the other hand, Schiff base S(II) with 4-amino acetanilide show a strong band at around 1,650 cm^{-1} that resulted from overlapping of carbonyl group characteristic band with the new generated one at 16,334.5 cm^{-1} attributed to –C=N vibration of Schiff bases. Furthermore, the presence of the amino group in the structure of 4-amino acetanilide increases the number of formed Schiff base with glutaraldehyde (GA).

3.1.2. Thermal analysis

TGA curves of Chitosan and the different derivatives were done and represented in Fig. 5. Chitosan and its derivatives show three different degradation rates. First depression that started from ambient temperature to approximately 150℃ that related to evaporation of moisture content attached to polymer chains [57,58]. A second depression, starting from 230℃ related to oxidative decomposition of Chitosan backbone. In this stage, depression was resulted from the destruction of amine groups in pyranose ring to form new cross-linked fragment. Third decomposition step, which appears at high temperature, may result from the thermal degradation of a new crosslinked material formed by thermal crosslinking reactions occurring in the first degradation process [58–60].

Decomposition shifts of the prepared derivatives with the native Chitosan recognized in Table 1. Chitosan classified as hydrophilic natural biopolymer; the presence of hydrophilic groups such as hydroxyl and amine groups is a primary reason for the presence of moisture combined with polymer chains [61]. The amount of water attached to polymer changed by the modification process as a new group introduced to its structure. In our Schiff bases, the coupling of 1-vinyl 2- pyrrolidone (I) and four amino acetanilide (II) with Chitosan amine groups showing an increase of moisture content with first derivative rather than decrease

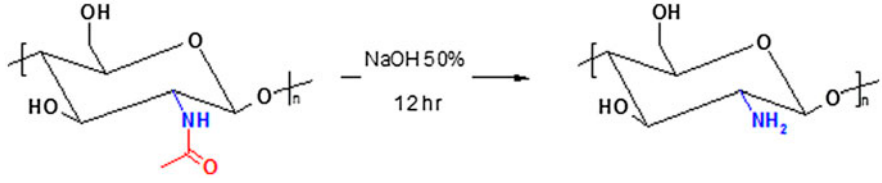

Fig. 1. Preparation of chitosan.

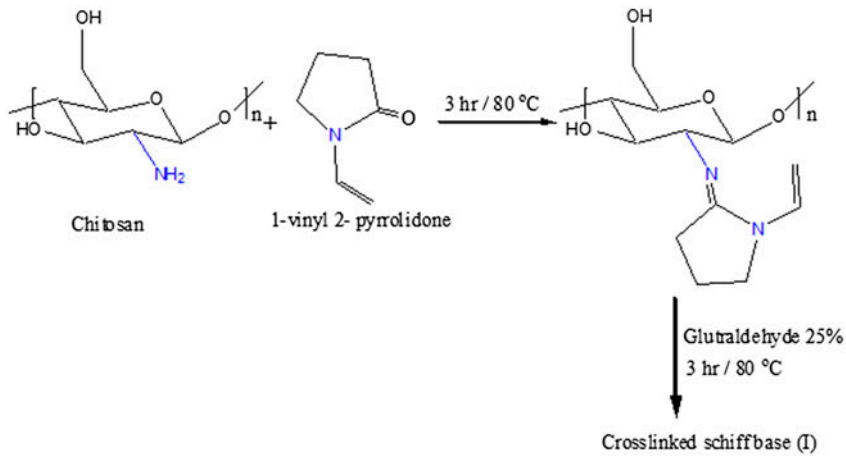

Fig. 2. Preparation of cross-linked Schiff base, S(I).

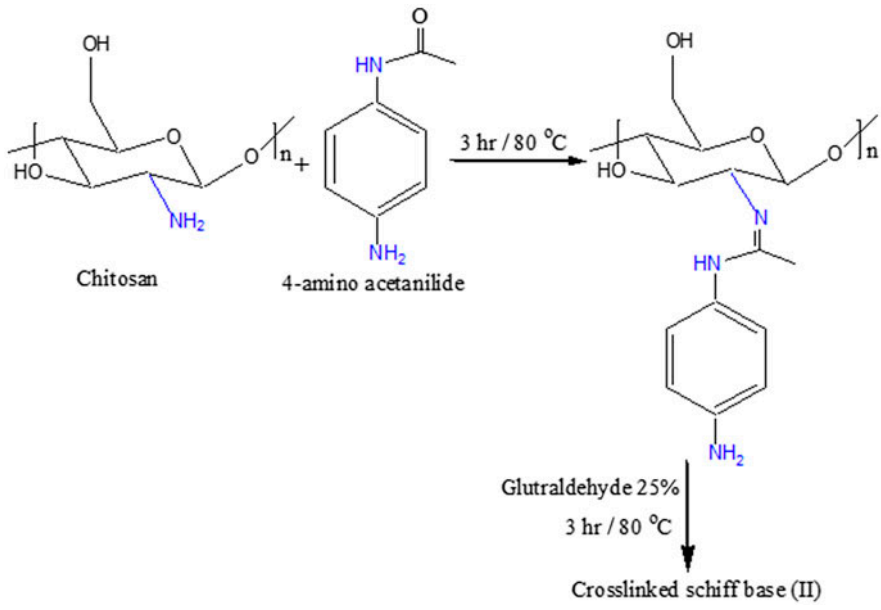

Fig. 3. Preparation of cross-linked Schiff base, S(II).

of the second derivative that refer to change in the hydrophilic character of produced derivative.

Chitosan Schiff bases (I) and (II) showed a higher thermal stability than Chitosan itself. Contrary to several previous studies recording a decrease of Chitosan Schiff base thermal stability, that attributed this lowering of thermal stability via replacement of $–NH_2$ with –N=C group [62,63]. Other studies agree with our obtained results, it record increase in thermal stability of Chitosan Schiff bases rather than Chitosan [64,65].

We expected that this depended on the type of the newly attached groups. In the present modification, connecting phenolic or vinyl groups to amine groups support structure with conjugated double bonds that are able to stabilize free radicals produced during thermal degradation. Evidence of suggested mechanism approved by the slow degradation in case of Schiff bases (I) and (II) rather than severe depression in Chitosan.

3.2. Batch adsorption experiments

3.2.1. Effect of contact time

To establish equilibrium time for maximum uptake and to know the kinetics of the adsorption process,

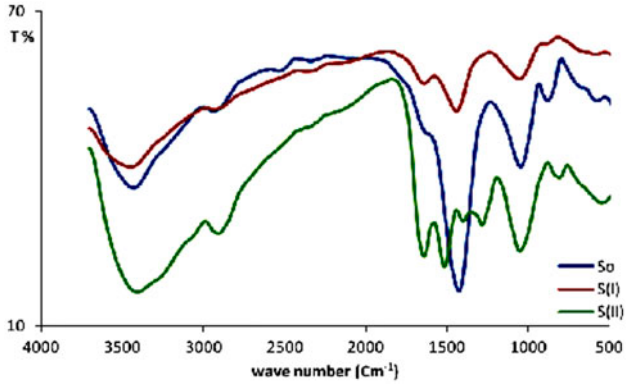

Fig. 4. FT-IR spectrum of Chitosan S(0) and two different Schiff bases (I) and (II).

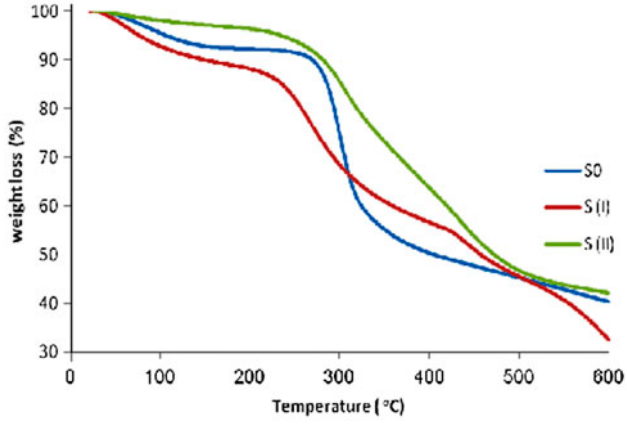

Fig. 5. Thermal gravimetric analysis of Chitosan S(0) and two different Schiff bases (I) and (II).

the adsorption of MO using the three Chitosan and Chitosan Schiff bases (I, II) studied as a function of contact time; Fig. 6.

The results show an increase in dye removal with time and attain an equilibrium within 70 min; this effect has arisen from the fact that the amount of dye uptake is a function of time [66–68]. Thus, 70 min is chosen as the reaction time required reaching equilibrium in the present MO sorption process. The figure shows an increase in removing the power of Schiff base (I) rather than Chitosan, where Schiff base (II) demonstrates less activity than parent Chitosan itself.

Chitosan has reactive amino and hydroxyl groups that interact with negatively charged surfaces. The behavior of Chitosan involves two factors, namely hydrophobic interactions and the possibility of chain association through hydrogen bridges. The hydrophobic interactions are due to the methyl group of the acetamide function and the –CH and $–CH_2$ groups of the glucose ring. The H-bridges usually generated by alcohol, amine, amide, and ether functions on the Chitosan chain. These chemical groups implied in the competitive formation of both inter- and intramolecular H-bridges, as well as interactions with other substrates. Thus, adsorption of anionic dye on Chitosan was done via chemical and physical sorption behavior [69–74], in the current modification, Schiff base (II) substitute active cationic amine groups with phenolic amine groups that less active.

3.2.2. Effect of initial dye concentration

Fig. 7 shows the effect of initial MO concentration on % removal. The removal percentage reduced with an increase in initial MO concentration at a fixed adsorbent dosage (0.1 g).

Furthermore, the results showed a linear increase in the removing capacity of polymers with increasing concentration of dye solution. This increment indicates that the initial dye concentrations play a significant role in the adsorption capacities of MO on Chitosan or Chitosan derivatives. Although the amount of the dye adsorbed increased with increasing concentration of the solution, the percentage of adsorption decreased. This trend is due to the electrostatic repulsion between the dye molecules with increasing concentration that results in a competition between the dye molecules for

Table 1
Peak temperature and weight loss of TGA analysis

	Piping water content Ambient-120°C Total loss (%)	1st stage depression Ambient-200°C Total loss (%)	2nd stage depression			2nd stage depression				
			T_{Start} (°C)	T_{End} (°C)	Total loss %	T_{Start} (°C)	T_{End} (°C)	Total loss (%)	T_{50} (°C)	Remaining at 600°C (%)
Chitosan (S_0)	21	8	267	342	36.4	342	600	15.85	405.9	40.35
Schiff Base (S_I)	26.79	12	233.7	424.9	32.17	424.9	600	22.83	457.5	32.55
Schiff Base (S_{II})	15.5	3.5	259	502	45.51	502	600	5.38	473	42.25

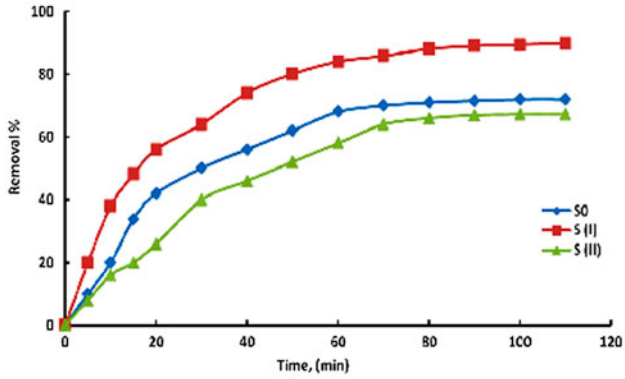

Fig. 6. Effect of contact time on the adsorption of methyl orange by the different prepared materials (initial dye conc. = 50 ppm; adsorbent dose = 0.1 g; solution volume, 25 ml, temperature = 25 ± 2˚C; agitation speed = 200 rpm; pH 7).

the limited active sites in the adsorbent. A similar effect observed with the other anionic dyes [3,43,71,73].

3.2.3. Effect of adsorbent dose

The effect of adsorbent dosage on MO adsorption was investigated by changing the adsorbent dosage from 0.1 to 0.4 g and equilibrated for 70 min at an initial dye concentration of 50 ppm; all experiments were carried out at the same stirring speed, 200 rpm. The results presented in Fig. 8. It is apparent that the % removal of methyl orange increased as adsorbent amount increased. This result was expected because, for a fixed initial dye concentration, increasing adsorbent amount provides greater surface area and sorption sites [74,75].

3.2.4. Effect of agitation speed on MO adsorption

To inspect the effect of stirring rate on MO adsorption, a series of batch experiments were carried out by mixing initial dye concentration of, 50 ppm with fixed amount of each ion exchanger (0.1 g) with different agitation speed from (0 to 250 rpm) illustrated in Fig. 9.

Results clearly depict that adsorption of MO increased as agitation speed increased. The reason may be that there is a stagnant flow layer existing on the adsorbent surface. According to published data [76], in adsorption systems, the stirring rate increase causes an increase in film diffusivity. This increase in film diffusivity facilitates dye diffusion, increasing adsorption capacity. The intraparticle diffusivity increase was a consequence only of adsorption capacity increase. Intraparticle diffusivity value largely depends on the surface properties of adsorbents and adsorption capacity. So increasing the stirring rate will reduce the thickness of the liquid film and the mass-transfer resistance to the three different Chitosan adsorbent surfaces. Therefore, the adsorption of MO will be increased with the degree of mixing [77–79].

3.2.5. Effect of solution pH

Solution pH is an important parameter that affects the adsorption of dye molecules, influencing not only the surface charge of the adsorbent, and the

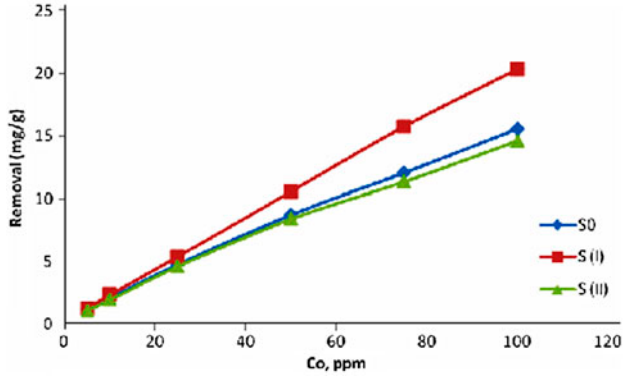

Fig. 7. Effect of initial concentration on the adsorption of MO by the different prepared adsorbents (Adsorbent dose = 0.1 g; solution volume, 25 ml, temperature = 25 ± 2˚C; contact time = 70 min; agitation speed = 200 rpm; pH 7).

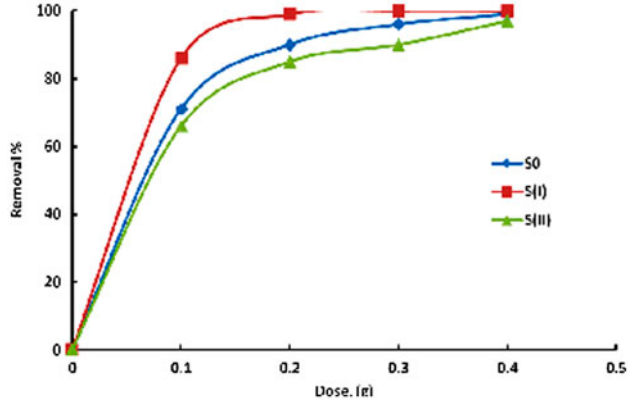

Fig. 8. Effect of adsorbent dose on the adsorption of methyl orange by the different prepared adsorbents (initial conc. = 50 ppm; solution volume, 25 ml, temperature = 25 ± 2˚C; contact time = 70 min; agitation speed = 200 rpm; pH 7).

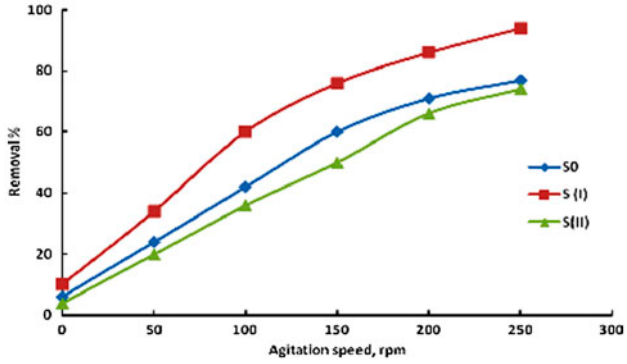

Fig. 9. Effect of agitation speed on the adsorption of methyl orange by the different prepared adsorbents (Adsorbent dose = 0.1 g; solution volume, 25 ml, temperature = 25 ± 2˚C; contact time = 70 min; pH 7).

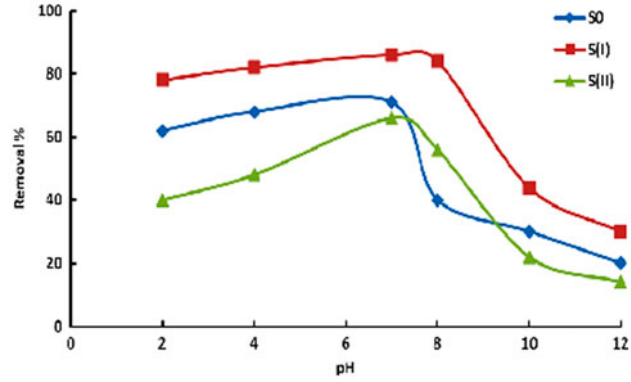

Fig. 10. Effect of pH on the adsorption of methyl orange by the different prepared adsorbents (Adsorbent dose = 0.1 g; solution volume, 25 ml, temperature = 25 ± 2˚C; contact time = 70 min; agitation speed = 200 rpm).

dissociation of functional groups on the active sites of the adsorbent, but also the chemistry of MO solution. The effect of variation the initial MO solution's pH on its adsorption presented in Fig. 10. In general, the uptakes are much higher in acidic solutions than those in neutral and alkaline conditions. At lower pH, more protons will be available to protonate amine groups of Chitosan molecules to form groups $-NH_3$, MO an acidic dye and contains negatively charged sulfonate group ($-SO_3^-Na^+$). Thereby increasing electrostatic attractions between dye molecules and adsorption sites and causing the observed increase in dye adsorption. This explanation agrees with our data on pH effect. It can be seen that the pH of aqueous solution plays a significant role in the adsorption of MO onto Chitosan and its derivatives. Similar results are previously published [68,80]. The adsorption capacities of Chitosan and Chitosan Schiff base (II) declined as a pH increase from 8.0 to 12.0. On the other hand, the adsorption capacity of Chitosan Schiff base (I) kept constant at pH 8. At alkaline, the surface charges of Chitosan beads are negative. That hinders the adsorption by the electrostatic force of repulsion between the negatively charged dye molecules and the adsorbent (Chitosan hydro-beads). However, the appreciable amount of dye removal in this pH range suggests the substantial involvement of other physical forces such as hydrogen bonding, van der Waals force, etc. in the adsorption process [72].

3.2.6. Effect of solution temperature

Experiments were carried out at the same initial MO concentration of 50 ppm, with an adsorbent dose of 0.1 g/25 mL to investigate the effect of temperature from 25 to 80˚C on MO adsorption. The results reveal that adsorption of dye gradually increased by increase temperature, Fig. 11. The curves indicate the strong tendency of the process for monolayer formation process to occur [41,69,81–86]. The temperature increment would increase the mobility of the large dye ions as well as produce a swelling effect on the internal structure of the Chitosan. That consequently facilitates the diffusion of the large dye molecules [86–89].

Therefore, the adsorption capacity should largely depend on the chemical interaction between the functional groups on the adsorbent surface and the adsorbate, and should increase as the temperature rises. That increment explained by a rise in the adsorbate diffusion rate into the pores. In an endothermic process, the adsorbent diffusion might contribute to the adsorption of MO (Reactive dye) at higher temperatures.

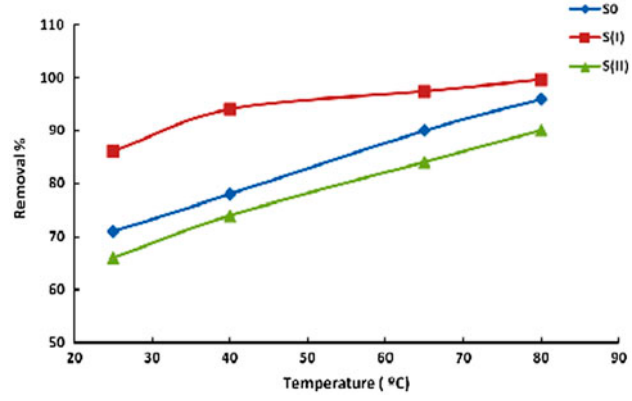

Fig. 11. Effect of temperature on the adsorption of MO by the different prepared adsorbents (Adsorbent dose = 0.1 g; solution volume, 25 ml; contact time = 70 min; agitation speed = 200 rpm; pH 7).

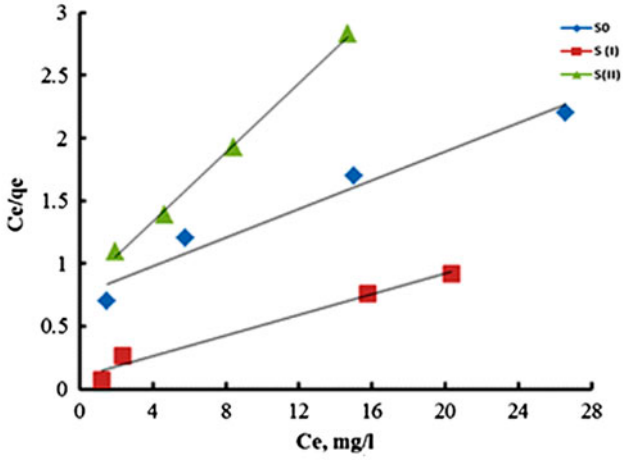

Fig. 12. Langmuir adsorption isotherm for MO adsorption using the three prepared adsorbents at various initial solution concentrations.

3.3. Adsorption isotherms

Equilibrium data permit evaluation of Chitosan and its Schiff bases adsorption properties as it describes how the adsorbate molecules interact with adsorbent molecules when the adsorption process reaches equilibrium. That provides a comprehensive understanding of the nature of the interaction. The Langmuir isotherm based on the assumption of monolayer adsorption on the surface containing a finite number of adsorption sites of uniform distribution and energies of adsorption. On the other hand, Freundlich isotherm postulates the heterogeneous nature of the adsorbent surface, reversible adsorption process and unlimited to monolayer adsorption. The surface area is the limiting factor in Langmuir isotherm that referred the maximum capacity to the saturation of the surface with a monolayer of adsorbate.

3.3.1. Langmuir isotherm

A plot of C_e/q_e vs. C_e should indicate a straight line of slope $1/q_m$ and an intercept of $1/q_m K$. Fig. 12 illustrates the linear plot of Langmuir equation for MO adsorption at various initial ions concentrations using the different prepared Chitosan adsorbents. From the correlation coefficient (R^2) values that regarded as a measure of the goodness-of-fit of experimental data on the isotherm's model. It indicated that the Langmuir equation represents the sorption process of MO at the prepared adsorbents very well; the R^2 values were all higher than 0.96, indicating a good mathematical fit.

Langmuir parameters for ions removal, q_m, and K were calculated from the slope and intercept of these figures and tabulated in Table 2.

Comparing the sorption parameters of the three prepared adsorbents for MO removal, it's clear that S (I) had the largest monolayer capacity than the two other samples for MO removal. Instead, the fact that S (II) has more formed Schiff sites, it adsorption capacity is less even than Chitosan itself. This unexpected result can refer to the high crosslinking degree between the Chitosan matrix and the coupled 4-aminoacetanilide. That reduced the diffusion of MO molecules to the entire pores surface and so the adsorbed amount. This postulation reinforced by the values of K_L (affinity of the binding sites); Table 2. From the table, it is clear that K_L value of S(II) is higher than S(0).

3.3.2. Freundlich isotherm

Fig. 13 investigates the linear regression approach for sorption MO using the three different prepared sorbents to obtain the model parameters of Freundlich isotherm. From this figure according to the correlation coefficient (R^2) values, it was confirmed that the removal of MO molecules using the different prepared Chitosan samples obeyed the Freundlich isotherm. The magnitude of $1/n$ quantifies the favorability of adsorption and the degree of heterogeneity on the surface of adsorbents. If $1/n$ is less than unity, suggesting favorable adsorption, then adsorption capacity increases and new adsorption sites will be formed [90]. Both S(0) and S(2) sorbents have a $1/n$ value less than unity while S(1) higher than unity. This data confirms the homogeneity of S(1) sorbent; Table 2.

Table 2
Langmuir and Freundlich sorption parameters for MO adsorption using the different prepared adsorbents

	S(0)			S(I)			S(II)		
Isotherm model	q_m (mg/g)	K (L/mg)	R^2	q_m (mg/g)	K (L/mg)	R^2	q_m (mg/g)	K (L/mg)	R^2
Langmiur Isotherm	1.3	13	0.96	10.7	2.3	0.98	1.2	5.9	0.99
Freundlich Isotherm	k_f	n	R^2	k_f	n	R^2	k_f	n	R^2
	1.7	1.9	0.94	1.8	0.9	0.98	1.5	3.8	0.94

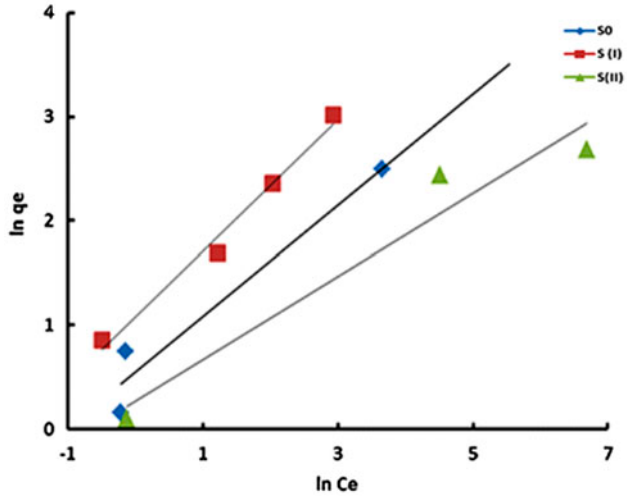

Fig. 13. Freundlich isotherm for MO sorption using the different prepared Chitosan sorbents at various initial solution concentrations.

Finally, it was found that Langmuir isotherm model fitted to the experimental data better than Freundlich isotherm model. The applicability of Langmuir isotherm suggested that the dye coverage on the surface of the prepared adsorbents is a monolayer. This conclusion is in agreement with many other published results [90–92].

3.4. Kinetic studies

Kinetics of the adsorption process governs the efficiency, the equilibrium time, and also investigates the rate of the adsorption process. Two kinetic models (pseudo-first-order and pseudo-second-order kinetics) used to recognize the possible rate-controlling steps involved in the process of adsorption.

3.4.1. Pseudo-first-order reaction kinetic

Simple linear equation for pseudo-first-order reaction kinetic are given below:

$$\ln (q_e - q_t) = \ln q_e - k_1 t \quad (6)$$

where k_1 is the rate constant of the first-order adsorption, q_t is the amount of MO adsorbed at time "t" (mg/g), and q_e is the amount of MO adsorbed at saturation (mg/g). The plot of ln (q_e/q_t) vs. t allows calculation of the rate constant k_1 and q_e for MO removal (Table 3).

3.4.2. Pseudo-second-order reaction kinetic

Pseudo-second-order reaction kinetic expressed as:

$$t/q_t = 1/k_2 q_e^2 + t/q_e \quad (7)$$

where k_2 (g/mg min) is the pseudo-second-order rate constant, q_e the amount adsorbed at equilibrium, and q_t is the amount of dye adsorbed at the time (t). Similar to the pseudo-first-order reaction kinetic, q_e and k_2 can be determined from the slope and intercepts of plot t/q_t vs. t (Table 4).

From the two previous tables (Tables 3 and 4), which summarize the calculated rate constants (k_1 and k_2), adsorbed amounts of MO per unit mass of each prepared Chitosan sample (q_e) and linear regression correlation coefficients (R^2) for pseudo-first- and -second-order reaction kinetics. It was clear that, in pseudo-first-order reaction kinetic, calculated values of q_e are closer to the experimental values for the three prepared adsorbents samples. Furthermore, correlation coefficients are higher for first-order kinetic studies.

Table 3
Comparison of adsorption rate constants, experimental, and calculated q_e values for the pseudo-first-reaction kinetics of removal of MO by the prepared nano-chitosan samples

Sample	Initial MO conc. (mg/l)	$q_{e,experimental}$ (mg/g)	K_1 (min^{-1})	$q_{e,calculated}$ (mg/g)	R^2
S0	50	9	0.040	8.9	0.99
	75	12	0.037	11.6	0.99
	100	15.8	0.035	15.7	0.99
S1	50	9	0.128	10.8	0.96
	75	12	0.075	12.9	0.98
	100	15.8	0.059	16.8	0.97
S2	50	9	0.04	8.6	0.97
	75	12	0.069	13	0.97
	100	15.8	0.035	17.8	0.98

Table 4
Comparison of adsorption rate constants, experimental, and calculated q_e values for the pseudo-second-reaction kinetics of removal of MO bye the different prepared adsorbents

Sample	Initial MO conc. (mg/L)	$q_{e,experimental}$ (mg/g)	K_2 (g/mg min)	$q_{e,calculated}$ (mg/g)	R^2
S0	50	9	0.008	9.8	0.93
	75	12	0.004	13.9	0.89
	100	15.8	0.001	21.3	0.77
S(I)	50	9	0.006	12.5	0.89
	75	12	0.003	17.5	0.88
	100	15.8	8×10^{-4}	31	0.67
S(II)	50	9	0.006	10.5	0.87
	75	12	0.004	14.7	0.89
	100	15.8	0.002	19.3	0.655

Table 5
Maximum monolayer adsorption capacities (q_m, mg/g) of MO on different adsorbents

Adsorbent	q_m (mg/g)	Refs.
pHEMA–CS-f-MWCNT com-posite	360	[91]
Zr (IV)- cross-linked chitosan/bentonite composite	438.6	[93]
Chitosan	30	[94]
Porous chitosan doped graphene oxide	687	[95]
Fe_3O_4/Al_2O_3/chitosan composite	416	[96]
Chitosan Schiff bases	20	This work

Thus, chemical adsorption is not the rate-limiting step of the adsorption mechanism. This result is in disagreement with many published results [91,93–96] which demonstrated that the kinetic of MO adsorption process fitted well with pseudo-second-order reaction kinetic. This disagreement can refer to many things. The difference between matrices in their chemical structure, porosity, and combined materials in case of composites. Consequently, this affects the adsorption capacity that shows higher values of matrices obeyed the pseudo-second-order reaction kinetic as shown in Table 5. Crosslinking of Chitosan matrices reduced the porous structure and so the available adsorption sites on their surface. The high MW nature of MO molecule reinforced this assumption.

4. Conclusion

Novel crosslinked Chitosan derivate Schiff bases developed by the coupling of Chitosan with 1-vinyl 2-pyrrolidone [Schiff base (I)] and 4-amino acetanilide [Schiff base (II)] for the adsorption of anionic reactive dye (Methyl orange) from aqueous solutions. The results showed an increase in the dye removal with time and attained the equilibrium within 70 min. Variation of the initial dye concentration reduced the removal percentage at a fixed adsorbent dosage (0.1 g). Furthermore, the results showed a linear increase in the removing capacity of polymers with increasing the initial dye concentration to reach 20 mg/g and 15 mg/g for S(I), S(0), and S(II), respectively. The results reveal that adsorption of dye gradually increased by increase temperature from 25 to 80˚C where the curves indicate the strong tendency of the process for monolayer formation. A decline of the adsorption capacities of Chitosan and Chitosan Schiff base (II) were observed at pH from 8.0 to 12. On the other hand, Chitosan Schiff base (I) kept constant adsorption capacity at pH 8. Results clearly depict that the adsorption of MO increased as agitation speed increase from 0 up to 250 rpm. It is apparent that the methyl orange removal % increased as the adsorbent amount rose from 0.1 to 0.4 g. Langmuir model was able to describe the equilibrium data and fitted perfectly. The experimental kinetics data clearly depict that the kinetics of the methyl orange dye removal using the prepared sorbents follows the pseudo-first-order model.

References

[1] I.M. Banat, P. Nigam, D. Singh, R. Marchant, Microbial decolorization of textile-dyecontaining effluents: A review, Bioresour. Technol. 58 (1996) 217–227.

[2] T. Robinson, G. McMullan, R. Marchant, P. Nigam, Remediation of dyes in textile effluent: A critical review on current treatment technologies with a proposed alternative, Bioresour. Technol. 77 (2001) 247–255.

[3] M.S. Chiou, H.Y. Li, Equilibrium and kinetic modeling of adsorption of reactive dye on cross-linked chitosan beads, J. Hazard. Mater. 93 (2002) 233–248.

[4] X.Y. Yang, B. Al-Duri, Application of branched pore diffusion model in the adsorption of reactive dyes on activated carbon, Chem. Eng. J. 83 (2001) 15–23.

[5] M.S. Mottaleb, D. Littlejohn, Application of an HPLC-FTIR modified thermospray interface for analysis of dye samples, Anal. Sci. 17 (2001) 429–434.

[6] S.M. Burkinshaw, O. Kabambe, Attempts to reduce water and chemical usage in the removal of bifunctional reactive dyes from cotton: Part 2 bis(vinyl sulfone), aminochlorotriazine/vinyl sulfone and bis (aminochlorotriazine/vinyl sulfone) dyes, Dyes Pigm. 88 (2011) 220–229.

[7] P.C. Vandevivere, R. Bianchi, W. Verstraete, Review: Treatment and reuse of wastewater from the textile wet-processing industry: Review of emerging technologies, J. Chem. Technol. Biotechnol. 72 (1998) 289–302.

[8] C. O'Neill, F.R. Hawkes, D.L. Hawkes, N.D. Lourenço, H.M. Pinheiro, W. Delée, Colour in textile effluents—Sources, measurement, discharge consents and simulation: A review, J. Chem. Technol. Biotechnol. 74 (1999) 1009–1018.

[9] Y. Ho, T. Chiang, Y. Hsueh, Removal of basic dye from aqueous solution using tree fern as a biosorbent, Process Biochem. 40 (2005) 119–124.

[10] F. Derbyshire, M. Jagtoyen, R. Andrews, A. Rao, I. MartinGullon, E. Grulke, Carbon materials in environmental applications, in: L.R. Radovic (Ed.), Chemistry and Physics of Carbon, vol. 27, Marcel Dekker, New York, NY, 2001, pp. 1–66.

[11] V. Vimonses, S. Lei, B. Jin, C.W.K. Chow, C. Saint, Adsorption of congo red by three Australian kaolins, Appl. Clay Sci. 43 (2009) 465–472.

[12] S.L. Bartelt-Hunt, S.E. Burns, J.A. Smith, Nonionic organic solute sorption onto two organobentonites as a function of organic-carbon content, J. Colloid Interface Sci. 266 (2003) 251–258.

[13] M. Akçay, G. Akçay, The removal of phenolic compounds from aqueous solutions by organophilic bentonite, J. Hazard. Mater. 113 (2004) 189–193.

[14] A.S. Özcan, B. Erdem, A. Özcan, Adsorption of Acid Blue 193 from aqueous solutions onto BTMA-bentonite, Colloids Surf. A: Physicochem. Eng. Aspects 266 (2005) 73–81.

[15] M. Özacar, İ. Ayhan Şengil, A two stage batch adsorber design for methylene blue removal to minimize contact time, J. Environ. Manage. 80 (2006) 372–379.

[16] A. Özcan, Ç. Ömeroğlu, Y. Erdoğan, A.S. Özcan, Modification of bentonite with a cationic surfactant: An adsorption study of textile dye Reactive Blue 19, J. Hazard. Mater. 140 (2007) 173–179.

[17] E. Alver, A.Ü. Metin, Anionic dye removal from aqueous solutions using modified zeolite: Adsorption kinetics and isotherm studies, Chem. Eng. J. 200–202 (2012) 59–67.

[18] Y. Benkli, M. Can, M. Turan, M. Çelik, Modification of organo-zeolite surface for the removal of reactive azo dyes in fixed-bed reactors, Water Res. 39 (2005) 487–493.

[19] N.N. Fathima, R. Aravindhan, J.R. Rao, B.U. Nair, Dye house wastewater treatment through advanced oxidation process using Cu-exchanged Y zeolite: A heterogeneous catalytic approach, Chemosphere 70 (2008) 1146–1151.

[20] E. Rosales, M. Pazos, M. Sanromán, T. Tavares, Application of zeolite-Arthrobacter viscosus system for the removal of heavy metal and dye: Chromium and Azure B, Desalination 284 (2012) 150–156.

[21] N. Sapawe, A. Jalil, S. Triwahyono, M. Shah, R. Jusoh, N. Salleh, B. Hameed, A. Karim, Cost-effective microwave rapid synthesis of zeolite NaA for removal of methylene blue, Chem. Eng. J. 229 (2013) 388–398.

[22] S. Sohrabnezhad, A. Pourahmad, Comparison absorption of new methylene blue dye in zeolite and nanocrystal zeolite, Desalination 256 (2010) 84–89.

[23] S. Wang, H. Li, S. Xie, S. Liu, L. Xu, Physical and chemical regeneration of zeolitic adsorbents for dye removal in wastewater treatment, Chemosphere 65 (2006) 82–87.

[24] S. Wang, H. Li, L. Xu, Application of zeolite MCM-22 for basic dye removal from wastewater, J. Colloid Interface Sci. 295 (2006) 71–78.

[25] S. Wang, Z. Zhu, Characterisation and environmental application of an Australian natural zeolite for basic dye removal from aqueous solution, J. Hazard. Mater. 136 (2006) 946–952.

[26] X.S. Wang, Y. Zhou, Y. Jiang, C. Sun, The removal of basic dyes from aqueous solutions using agricultural by-products, J. Hazard. Mater. 157 (2008) 374–385.

[27] M. Doğan, H. Abak, M. Alkan, Biosorption of methylene blue from aqueous solutions by hazelnut shells: Equilibrium, parameters and isotherms, Water Air Soil Pollut. 192 (2008) 141–153.

[28] A.R. Khan, H. Tahir, F. Uddin, U. Hameed, Adsorption of methylene blue from aqueous solution on the surface of the wool fiber and cotton fiber, J. Appl. Sci. Environ. Manage. 9 (2005) 29–35.

[29] A. Mittal, J. Mittal, A. Malviya, D. Kaur, V. Gupta, Adsorption of hazardous dye crystal violet from wastewater by waste materials, J. Colloid Interface Sci. 343 (2010) 463–473.

[30] A.L. Prasad, T. Santhi, Adsorption of hazardous cationic dyes from aqueous solution onto Acacia nilotica leaves as an eco-friendly adsorbent, Sustain. Environ. Res. 22 (2012) 113–122.

[31] P. Sudamalla, P. Saravanan, M. Matheswaran, Optimization of operating parameters using response surface methodology for adsorption of crystal violet by activated carbon prepared from mango kernel, Environ. Res. 22 (2012) 1–7.

[32] J. Torres-Pérez, M. Solache-Ríos, A. Colín-Cruz, Sorption and desorption of Dye rem azole yellow onto a Mexican surfactant-modified clinoptilolite-rich stuff and a carbonaceous material from pyrolysis of sewage sludge, Water Air Soil Pollut. 187 (2008) 303–313.

[33] X. Wang, Invasive freshwater macrophyte alligator weed: Novel adsorbent for removal of malachite green from aqueous solution, Water Air Soil Pollut. 206 (2010) 215–223.
[34] G. Crini, Non-conventional low-cost adsorbents for dye removal: A review, Bioresour. Technol. 97 (2006) 1061–1085.
[35] L.D. Fiorentin, D.E.G. Trigueros, A.N. Módenes, F.R. Espinoza-Quiñones, N.C. Pereira, S.T.D. Barros, O.A.A. Santos, Biosorption of reactive blue 5G dye onto drying orange bagasse in batch system: Kinetic and equilibrium modeling, Chem. Eng. J. 163 (2010) 68–77.
[36] C.P. Kaushik, R. Tuteja, N. Kaushik, J.K. Sharma, Minimization of organic chemical load in direct dyes effluent using low cost adsorbents, Chem. Eng. J. 155 (2009) 234–240.
[37] G.Z. Kyzas, A decolorization technique with spent "Greek Coffee" Grounds as zero-cost adsorbents for industrial textile wastewaters, Materials 5 (2012) 2069–2087.
[38] G.Z. Kyzas, M. Kostoglou, A.A. Vassiliou, N.K. Lazaridis, Treatment of real effluents from dyeing reactor: Experimental and modeling approach by adsorption onto chitosan, Chem. Eng. J. 168 (2011) 577–585.
[39] G.Z. Kyzas, N.K. Lazaridis, A.C. Mitropoulos, Removal of dyes from aqueous solutions with untreated coffee residues as potential low-cost adsorbents: Equilibrium, reuse and thermodynamic approach, Chem. Eng. J. 189–190 (2012) 148–159.
[40] R.S. Juang, R.L. Tseng, F.C. Wu, S.H. Lee, Adsorption behavior of reactive dyes from aqueous solutions on chitosan, J. Chem. Technol. Biotechnol. 70 (1997) 391–399.
[41] D. Knorr, Dye binding properties of chitin and chitosan, J. Food Sci. 48 (1983) 36–37.
[42] G. Annadurai, L.Y. Ling, J.F. Lee, Adsorption of reactive dye from an aqueous solution by chitosan: Isotherm, kinetic and thermodynamic analysis, J. Hazard. Mater. 152 (2008) 337–346.
[43] S. Chatterjee, S. Chatterjee, B.P. Chatterjee, A.K. Guha, Adsorptive removal of congo red, a carcinogenic textile dye by chitosan hydrobeads: Binding mechanism, equilibrium and kinetics, Colloids Surf., A: Physicochem. Eng. Aspects 299 (2007) 146–152.
[44] F.A.A. Tirkistani, Thermal analysis of some chitosan Schiff bases, Polym. Degrad. Stab. 60 (1998) 67–70.
[45] J.E. dos Santos, E.R. Dockal, É.T.G. Cavalheiro, Synthesis and characterization of Schiff bases from chitosan and salicylaldehyde derivatives, Carbohydr. Polym. 60 (2005) 277–282.
[46] A.M. Donia, A.A. Atia, K.Z. Elwakeel, Selective separation of mercury(II) using magnetic chitosan resin modified with Schiff's base derived from thiourea and glutaraldehyde, J. Hazard. Mater. 151 (2008) 372–379.
[47] H.M. Zalloum, Z. Al-Qodah, M.S. Mubarak. Copper adsorption on chitosan—Derived schiff bases, J. Macromol. Sci., Part A 46 (2008) 46-57.
[48] M.M. Islam, S.M. Masum, M.M. Rahman, M.A.I. Molla, A.A. Shaikh, S.K. Roy, Preparation of chitosan from shrimp shell and investigation of its properties, Int. J. Basic Appl. Sci. 11 (2011) 1–9.
[49] G. Rigby, Patent Substantially Undegraded Deacetylated Chitin and Processes for Producing the Same, USA 2,040,879, (1936) 1–7.
[50] E.A. Soliman, S.M. El-Kousy, H.M. Abd-Elbary, A.R. Abou-zeid, Low molecular weight chitosan-based schiff bases: Synthesis, characterization and antibacterial activity, Am. J. Food Technol. 8 (2013) 17–30.
[51] I. Langmuir, The adsorption of gases on plane surfaces of glass, mica and platinum, J. Am. Chem. Soc. 40 (1918) 1361–1403.
[52] M.S. Elgeundi, Colour removal from textile effluents by adsorption techniques, Water Res. 25 (1991) 271–273.
[53] K.S. Low, C.K. Lee, Quaternized rice husk as sorbent for reactive dyes, Bioresour. Technol. 61 (1997) 121–125.
[54] Z. Aksu, Biosorption of reactive dyes by dried activated sludge: Equilibrium and kinetic modelling, Biochem. Eng. J. 7 (2001) 79–84.
[55] C. Namasivayam, D. Kavitha, Removal of Congo Red from water by adsorption onto activated carbon prepared from coir pith, an agricultural solid waste, Dyes Pigm. 54 (2002) 47–58.
[56] H. Freundlich, Adsorption in solution, Z. Phys. Chemie 57 (1906) 384–470.
[57] A. Pawlak, M. Mucha, Thermogravimetric and FTIR studies of chitosan blends, Thermochim. Acta 396 (2003) 153–166.
[58] J. Zawadzki, H. Kaczmarek, Thermal treatment of chitosan in various conditions, Carbohydr. Polym. 80 (2010) 394–400.
[59] K. Sreenivasan, Thermal stability studies of some chitosanmetal ion complexes using differential scanning calorimetry, Polym. Degrad. Stab. 52 (1996) 85–87.
[60] F.S. Kittur, K.V. Harish Prashanth, K. Udaya Sankar, R.N. Tharanathan, Characterization of chitin, chitosan and their carboxymethyl derivatives by differential scanning calorimetry, Carbohydr. Polym. 49 (2002) 185–193
[61] R. Riham, A.M. Fekry, Antimicrobial and anticorrosive activity of adsorbents based on chitosan schiff's base, Int. J. Electrochem. Sci. 6 (2011) 2489–2508.
[62] M. Diab, A. El-Sonbati, M. Al-Halawany, D. Bader, Thermal stability and degradation of chitosan modified by cinnamic acid, Open J. Polym. Chem. 02 (2012) 14–20.
[63] W. Sajomsang, S. Tantayanon, V. Tangpasuthadol, M. Thatte, W.H. Daly, Synthesis and characterization of N-aryl Chitosan derivatives, Int. J. Biolog. Macromol. 43 (2008) 79–87.
[64] S. Sashikala, S. Syed Shafi, Synthesis and characterization of chitosan schiff base derivatives, Der. Pharm. Lett. 6 (2014) 90-97.
[65] T.F. Jiao, J. Zhou, J. Zhou, L. Gao, Y. Xing, X. Li, Synthesis and characterization of chitosan-based schiff base compounds with aromatic substituent groups, Iran. Polym. J. 20 (2011) 123–136.
[66] R. Aravindhan, N.N. Fathima, J.R. Rao, B.U. Nair, Equilibrium and thermodynamic studies on the removal of basic black dye using calcium alginate beads, Colloids Surf., A: Physicochem. Eng. Aspects 299 (2007) 232–238.
[67] M.S. Mohy Eldin, S.A. El-Sakka, M.M. El-Masry, I.I. Abdel-Gawad, S.S. Garybe, Removal of methylene blue dye from the aqueous medium by nano polyacrylonitrile particles, Desalin. Water Treat. 44 (2012) 1–3.
[68] G.L. Dotto, L.A.A. Pinto, Adsorption of food dyes onto chitosan: Optimization process and kinetic, Carbohydr. Polym. 84 (2011) 231–238.

[69] H. Yoshida, A. Okamoto, T. Kataoka, Adsorption of acid dye on cross-linked chitosan fibers: Equilibria, Chem. Eng. Sci. 48 (1993) 2267–2272.
[70] F.C. Wu, R.L. Tseng, R.S. Juang, Comparative adsorption of metal and dye on flake- and bead-types of chitosans prepared from fishery wastes, J. Hazard. Mater. 73 (2000) 63–75.
[71] M.S. Chiou, H.O. Pang-Yen, H.-Y. Li, Adsorption of anionic dyes in acid solutions using chemically cross-linked chitosan beads, Dyes Pigm. 60 (2004) 69–84.
[72] E. Assaad, A. Azzouz, D. Nistor, A.V. Ursu, T. Sajin, D.N. Miron, F. Monette, P. Niquette, R. Hausler, Metal removal through synergic coagulation–flocculation using an optimized chitosan–montmorillonite system, Appl. Clay Sci. 37 (2007) 258–274.
[73] A. Szyguła, E. Guibal, M.A. Palacın, M. Ruiz, A.M. Sastre, Removal of an anionic dye (Acid Blue 92) by coagulation–flocculation using chitosan, J. Environ. Manage. 90 (2009) 2979–2986.
[74] M. Salman, M. Athar, U. Shafique, R. Rehman, S. Ameer, S.Z. Ali, M. Azeem, Removal of formaldehyde from aqueous solution by adsorption on kaolin and bentonite: A comparative study, Turk. J. Eng. Environ. Sci. 36 (2012) 263–270.
[75] H. Hou, R. Zhou, P. Wu, L. Wu, Removal of Congo red dye from aqueous solution with hydroxyapatite/chitosan composite, Chem. Eng. J. 211–212 (2012) 336–342.
[76] D.M. Ruthven, Principles of Adsorption and Adsorption Processes, John Wiley & Sons, New York, NY, 1984.
[77] I. Uzun, Kinetics of the adsorption of reactive dyes by chitosan, Dyes Pigm. 70 (2006) 76–83.
[78] W.J. Weber, J.C. Morris, Kinetics of adsorption of carbon from solutions, J. Sanit. Eng. Div. Am. Soc. Civ. Eng. 89 (1963) 31–63.
[79] B. Noroozi, G.A. Sorial, H. Bahrami, M. Arami, Equilibrium and kinetic adsorption study of a cationic dye by a natural adsorbent—Silkworm pupa, J. Hazard. Mater. 139 (2007) 167–174.
[80] M.N.V.R. Kumar, A review of chitin and chitosan applications, React. Funct. Polym. 46 (2000) 1–27.
[81] E.O. Augustine, S.H. Yuh, Equilibrium sorption of anionic dye from aqueous solution by palm kernel fiber as sorbent, Dyes Pigm. 74 (2007) 60–66.
[82] G. McKay, G. Ramprasad, P.P. Mowli, Equilibrium studies for the adsorption of dyestuffs from aqueous solutions by low-cost materials, Water Air Soil Pollut. 29 (1986) 273–283.
[83] Y. Ho, T. Chiang, Y. Hsueh, Removal of basic dye from aqueous solution using tree fern as a biosorbent, Process Biochem. 40 (2005) 119–124.
[84] H. Yoshida, S. Fukuda, O. Okamoto, T. Kataoka, Recovery of a direct dye and acid dye by adsorption on Chitosan fiber—Equilibria, Water Sci. Technol. 23 (1991) 1667–1676.
[85] Y.C. Wong, Y.S. Szeto, W.H. Cheung, G. McKay, Adsorption of acid dyes on chitosan—Equilibrium isotherm analyses, Process Biochem. 39 (2004) 695–704.
[86] G. Gibbs, J.M. Tobin, E. Guibal, Influence of Chitosan pre-protonation on reactive black five sorption isotherm and kinetics, Ind. Eng. Chem. Res. 43 (2004) 1–11.
[87] A.W. Adamson, Physical Chemistry of Surface, Interscience Publishers Inc, New York, NY, 1960.
[88] L.Y. Fraiji, D.M. Hayes, T.C. Werner, Static and dynamic fluorescence quenching experiments for the physical chemistry laboratory, J. Chem. Educ. 69 (1992) 424–428.
[89] S.M. Venkat, D.M. Indra, C.S. Vimal, Use of bagasse fly ash as an adsorbent for the removal of brilliant green dye from aqueous solution, Dyes Pigm. 73 (2007) 269–278.
[90] Y. Yao, H. Bing, X. Feifei, C. Xiaofeng, Equilibrium and kinetic studies of methyl orange adsorption on multiwalled carbon nanotubes, Chem. Eng. J. 170 (2011) 82–89.
[91] H. Mahmoodian, O. Moradi, I. Tyagi, A. Maity, M. Asif, V.K. Gupta, Enhanced removal of methyl orange from aqueous solutions by polyHEMA–chitosan-MWCNT nano-composite, J. Mol. Liquids 202 (2015) 189–198.
[92] R. Deepika, M. Venkatesh Prabhu, M. Nandi Devi, Studies on the behavior of reactive dyes onto the cross-linked chitosan using adsorption isotherms, Int. J. Environ. Sci. 4 (2013) 323–351.
[93] L. Zhang, P. Hu, J. Wang, Q. Liu, R. Huang, Adsorption of methyl orange (MO) by Zr (IV)-immobilized cross-linked chitosan/bentonite composite, Int. J. Biol. Macromol. 81 (2015) 818–827.
[94] T.K. Saha, N.C. Bhoumik, S. Karmaker, M.G. Ahmed, H. Ichikawa, Y. Fukumori, Adsorption of methyl orange onto chitosan from aqueous solution, J. Water Resour. Prot. 2 (2010) 898–906.
[95] Y. Wang, G. Xia, C. Wu, J. Sun, R. Song, W. Huang, Porous chitosan doped with graphene oxide as highly effective adsorbent for methyl orange and amido black 10B, Carbohydr. Polym. 115 (2015) 686–693.
[96] B. Tanhaei, A. Ayati, M. Lahtinen, M. Sillanpää, Preparation and characterization of a novel chitosan/Al_2O_3/magnetite nanoparticles composite adsorbent for kinetic, thermodynamic and isotherm studies of Methyl Orange adsorption, Chem. Eng. J. 259 (2015) 1–10.